# Assessment of the Thermochemical Properties of Actinides in Molten Chlorides

Patrick I. Masset[a,b], Christos Apostolidis[a], Rikard Malmbeck[a], Jean Rebizant[a],
Jérôme Serp[a], and Jean-Paul Glatz[a]

[a] European Commission, Joint Research Centre, Institute for Transuranium Elements,
P. O. Box 2340, D-76125 Karlsruhe, Germany
[b] Present address: Karl Winnacker Institut der Dechema e. V., Theodor-Heuss Allee 25,
D-60486 Frankfurt am Main, Germany

Reprint requests to P. I. M.; Fax: + 49 69 7564-362/388; E-mail: masset@dechema.de

Z. Naturforsch. **63a,** 107 – 113 (2008); received April 3, 2007

*Presented at the EUCHEM Conference on Molten Salts and Ionic Liquids, Hammamet, Tunisia, September 16 – 22, 2006.*

The electrochemical properties of the chlorides of the actinides U, Pu, Np and Am ($AnCl_3$) were investigated by transient electrochemical techniques in the LiCl-KCl eutectic at 400 – 550 °C. The diffusion coefficients of the cations and the apparent standard potentials of the redox systems on an inert W electrode were measured. The Gibbs energy of dilute solutions of $AnCl_3$ as well as the activity coefficients were derived from electrochemical measurements. In addition, the electrochemical behaviour of the actinides on an Al electrode was investigated. They formed $AnAl_4$ alloys, the formation potentials of which allowed a quantitative recovery of the actinides and their separation from fission products and especially from lanthanides. In addition, the thermochemical properties of the $AnAl_4$ alloys were determined by electrochemical measurements.

*Key words:* Actinides; Thermochemical Properies; Molten Salts; Al Electrode; Pyrochemistry.

## 1. Introduction

As an alternative to aqueous reprocessing, pyrochemical reprocessing was envisaged to recover actinides (An) from spent nuclear fuel. Electrorefining was tested in a process where the actinides were group-separated from the bulk fission products in a molten salt electrolyte [1 – 3]. This necessitates the knowledge of the basic properties of the metallic cation in molten salts, e. g. diffusion coefficients, apparent standard potentials, and activity coefficients. The first studies on the electrochemical properties of actinides in molten salts started during the 50s with of uranium in many chloride-based melts: for example $MgCl_2$-NaCl-KCl, NaCl-KCl, LiCl-NaCl-$CaCl_2$-$BaCl_2$ and in the LiCl-KCl eutectic (see reviewed data in [4]). It was followed by the investigation of plutonium-based solutions in molten chlorides [5 – 7]. Later Martinot reported the apparent standard potentials of the redox systems of the actinide series (U, Pu, Np, Am, Cm) [7]. In the last decade re-assessments of the thermochemical properties of actinide chloride solutions have been undertaken: U [4, 8 – 13], Pu [10, 14, 15], Am [10, 16 – 21], Np [10, 22 – 24]. Also at the Institute for Transuranium Elements (ITU), Karlsruhe, Germany, systematic electrochemical studies on actinides in the molten eutectic LiCl-KCl have been initiated. The aim of these investigations is to provide sufficient experimental data to construct a process flow-sheet of a separation process of higher actinides as part of a molten salt recycling strategy. The present paper summarizes several investigations on the electrochemical behaviour of actinides in the LiCl-KCl eutectic with different electrodes:

- W (tungsten) electrode: as inert electrode it has been used for the study of the basic electrochemical behaviour of each element separately.
- Al (aluminium) electrode: as a reactive electrode it forms stable $AnAl_x$-type alloys. Al is a potential electrode material for the actinide separation [25].

## 2. Experimental

### 2.1. Chemicals

Chemicals and electrode preparation have already been reported [11]. Only the preparation

Table 1. Analytical expressions of the diffusion coefficients of $An^{p+}$ ($p = 2, 3, 4$) in the molten LiCl-KCl eutectic in the temperature range 400 – 550 °C.

| Ion | $D$ / cm$^2$ s$^{-1}$ | Ref. |
|---|---|---|
| $U^{3+}$ | $13.7 \cdot 10^{-4} \exp\{-24.2 \cdot 10^3/RT(\mathrm{K})\}$ | [4] |
| $U^{4+}$ | $5.25 \cdot 10^{-4} \exp\{-19.8 \cdot 10^3/RT(\mathrm{K})\}$ | [4] |
| $Np^{3+}$ | $9.47 \cdot 10^{-4} \exp\{-23.6 \cdot 10^3/RT(\mathrm{K})\}$ | [22] |
| $Np^{4+}$ | $2.14 \cdot 10^{-4} \exp\{-14.1 \cdot 10^3/RT(\mathrm{K})\}$ | [22] |
| $Pu^{3+}$ | $1.255 \cdot 10^{-2} \exp\{-40.2 \cdot 10^3/RT(\mathrm{K})\}$ | [14] |
| $Am^{3+}$ | $1.386 \cdot 10^{-2} \exp\{-40 \cdot 10^3/RT(\mathrm{K})\}$ | [17] |
| $Am^{2+}$ | $1.721 \cdot 10^{-2} \exp\{-44.75 \cdot 10^3/RT(\mathrm{K})\}$ | [17] |

of the actinide solutions is described in this paper.

$AnCl_3$ were prepared directly in the LiCl-KCl melt by oxidizing the corresponding An metal (plutonium: $^{239}$Pu-95%-$^{240}$Pu-4.6%, low Am content; uranium: depleted U; americium: high purity $^{241}$Am, > 99%). The actinide metal was introduced in a molten metallic pool (Cd or Bi) on the bottom of the crucible, and then oxidized by adding either $CdCl_2$ or $BiCl_3$ to the salt phase. The exchange reaction between the metallic and the salt phases occurs as follows:

$$n\,\mathrm{An}^0(\text{metallic phase}) + 3\mathrm{M}^{n+}(\text{salt phase}) \rightleftharpoons n\,\mathrm{An}^{3+}(\text{salt phase}) + 3\mathrm{M}^0,$$

where M denotes a metallic element (M = Cd, Bi) and $n$ is the oxidation state of M in the salt phase. By this method, a quantified amount of $An^{3+}$ could be released in the salt phase.

For neptunium-based experiments, $NpCl_4$ and $NpCl_3$ were used as starting materials. They were previously synthetized from $NpO_2$ according the method of Landreau. Details of the synthesis and Np-based solution preparation are given in [22].

### 2.2. Apparatus

The electrochemical experiments, storage and handling of all chemicals were carried out in a glove box under purified argon atmosphere (less than 5 ppm of water and 10 ppm of oxygen). Description and details of the cell arrangement can be found in [22].

### 2.3. Techniques

Transient electrochemical techniques, i. e. cyclic voltammetry (CV) and chronopotentiometry (CP), were carried out in an electrochemical cell with a three-electrode set-up. The measurements were performed using a Princeton Applied Research PAR 273 potentiostat with EG&G M270 electrochemical software. For semi-integral analysis of cyclic voltammograms by the convolution method (CM), the Condecon software was used. Samples (about 100 mg) were taken from the salt phase and dissolved in 1 M nitric acid. The concentration of actinide and the isotopic ratio were determined by ICP-MS analysis and by non-destructive analysis specially developed for pyrochemical samples.

## 3. Results and Discussion

### 3.1. Electrochemical Properties on an Inert W Electrode

#### Diffusion Coefficients

The diffusion coefficients were determined at different temperatures either by chronopotentiometry from Sand's law

$$i\tau^{1/2} = 0.5nFCS(\pi D)^{1/2}, \tag{1}$$

or by cyclic voltammetry using the Randles-Sevick relation

$$I_p/v^{1/2} = \beta(nF)^{3/2}C(RT)^{-1/2}SD^{1/2}, \tag{2}$$

where $\beta$ is equal to 0.446 or 0.61 if the transition is being considered as soluble-soluble or insoluble-soluble, respectively. In addition, the diffusion coefficients, $D$, of the actinide species were also derived from the convolution of cyclic voltammograms according to Saveant's technique

$$m = 1/\pi^{1/2}\int_0^t i(u)/(t-u)^{1/2}\mathrm{d}u, \tag{3}$$

using the limiting current

$$m^* = 3FSCD^{1/2}. \tag{4}$$

The values of the diffusion coefficients of the actinides are summarized in Table 1. They range between 1 and $5 \cdot 10^{-5}$ cm$^2$ s$^{-1}$ in the temperature range 400 – 550 °C. Despite the large size of the actinide cations their motion ability is comparable to other trivalent cations in the LiCl-KCl eutectic and should not be a barrier to the electrolysis process.

#### Apparent Standard Potentials

The apparent standard potential is the most important feature of the pyrochemical process as it deter-

Table 2. Analytical expressions of the apparent standard potentials of $An^{3+}/An^0$ (An = U, Np, Pu, Am) in the molten LiCl-KCl eutectic valid in the temperature range 400 – 550 °C.

| Redox system | | $E^{\circ *}$/V vs. $Cl_2/Cl^-$ | Ref. |
|---|---|---|---|
| U | $U^{3+}/U^0$ | $-3.099+0.0007689\ T(K)$ | [4] |
| | $U^{4+}/U^{3+}$ | $-1.902+0.0006104\ T(K)$ | [4] |
| Np | $Np^{3+}/Np^0$ | $-3.250+0.0007251\ T(K)$ | [22] |
| | $Np^{4+}/Np^{3+}$ | $-1.250+0.0006637\ T(K)$ | [22] |
| Pu | $Pu^{3+}/Pu^0$ | $-3.304+0.0006908\ T(K)$ | [14] |
| Am | $Am^{3+}/Am^{2+}$ | $-3.208+0.0006959\ T(K)$ | [17] |
| | $Am^{2+}/Am^0$ | $-3.279+0.0005016\ T(K)$ | [17] |

mines the separation of one actinide from another or the separation of actinides from the lanthanides. The apparent standard potentials were derived from chronopotentiometry and cyclic voltammetry measurements as well as by convolution techniques (semi-integration or semi-derivation). The equations to determine the apparent standard potential from different electrochemical techniques have already been reported in previous publications [4, 14, 17, 22] and are not described in this paper. Further details about the calculations can be found in books dedicated to electrochemical techniques. The equations describing the dependance of the apparent standard potentials on the temperature are reported in Table 2.

The main conclusions from these measurements are:

- the evolution of the apparent standard potential with the temperature is linear;
- the reduction of actinide anions $An^{3+}$ to actinide metal proceeds through one step except for Am (formation of $Am^{2+}$) which makes its recovery on an inert electrode difficult due to a disproportionation reaction;
- in the LiCl-KCl eutectic, the oxidation state +4 was observed only for U and Np;
- from the actinide reduction potential, W may be envisaged as electrode, but quantitative recovery remains difficult for Am and even for Pu when $U^{3+}$ is present in the melt; this could be overcome by using an Al-based electrode.

| Ion | $\gamma \cdot 10^3$ | Ref. |
|---|---|---|
| $U^{3+}$ | 1.4 | [4] |
| $U^{4+}$ | 14.8 | [4] |
| $Np^{3+}$ | 0.03 | [22] |
| $Np^{4+}$ | $4.9^a$ | [22] |
| $Pu^{3+}$ | $9.5^b$ | [14] |
| $Am^{3+}$ | $4.7^b$ | [17] |
| $Am^{2+}$ | $4.3^b$ | [17] |

Table 4. Activity coefficients of actinoide species in the LiCl-KCl eutectic at 500 °C.

[a] at 748 K.
[b] at 733 K.

### Thermochemical properties

From the apparent standard potential measurements the activity coefficients of the actinide species in the LiCl-KCl eutectic versus the temperature were deduced:

$$\Delta G^{\infty}(MCl_x) = -(p-q)FE^{\circ *}(M^{p+}/M^{q+}). \quad (5)$$

The activity coefficients of $MCl_x$, $\gamma_{MCL_x}$, in the LiCl-KCl eutectic were calculated from the difference between the Gibbs energy of formation at infinite dilution (determined from electrochemical measurements) and the Gibbs energy of formation in the supercooled state (sc) (see data from reference [26] in Table 3) taken as reference state:

$$RT\ln\gamma(MCl_x) = \Delta G^{\infty}(MCl_x) - \Delta G^{\circ}_{sc}(MCl_x). \quad (6)$$

The values of the activity coefficients of the actinide species as a function of the temperature are reported in Table 4. For $Np^{3+}$ and $U^{4+}$ the activity coefficients are close to $10^{-3}$. In any case the actinide-based solutions do not behave like ideal solutions. Strong local interactions might take place and significantly modify the structure of the melt at the local scale. For $Np^{3+}$ und $U^{4+}$ the activity coefficients range between $10^{-6}$ and $10^{-5}$. These values are in agreement with measurements carried out by other research groups [10 – 12].

Table 3. Selected thermodynamic properties for $AnCl_x$ compounds.

| Compound | $\Delta_f H^\circ$ / kJ mol$^{-1}$ | $S^\circ$ / J K$^{-1}$ mol$^{-1}$ | $C_p$(cr) / J K$^{-1}$ mol$^{-1}$ | $T_{fus.}$ / K | $\Delta_{fus.}H^\circ$ / kJ mol$^{-1}$ | $C_p$(liq.) / J K$^{-1}$ mol$^{-1}$ |
|---|---|---|---|---|---|---|
| $UCl_3$ | $-863.7 \pm 2.5$ | $163.9 \pm 0.5$ | $87.779 + 31.12 \cdot 10^{-3}(T/K) + 458.33 \cdot 10^3/(T/K)^{-2}$ | 1115 | 49 | 150 |
| $UCl_4$ | $-1019.8 \pm 2.5$ | $197.2 \pm 0.8$ | $106.854 + 48.65 \cdot 10^{-3}(T/K) - 89.603 \cdot 10^3/(T/K)^{-2}$ | 863 | 49.8 | 162.34 |
| $NpCl_3$ | $-896.8 \pm 2.5$ | $165.2 \pm 0.8$ | $89.598 + 27.5 \cdot 10^{-3}(T/K) + 83.712/(T/K)^{-2}$ | 1075 | 50 | 137 |
| $PuCl_3$ | $-959.6 \pm 2.5$ | $161.4 \pm 0.8$ | $91.412 + 37.16 \cdot 10^{-3}(T/K) + 27.38 \cdot 10^3/(T/K)^{-2}$ | 1041 | 49 | 144 |
| $AmCl_2$ | $-654.0 \pm 2.5$ | $148.1 \pm 0.8$ | ($\alpha$ phase) $64.992 + 24.57 \cdot 10^{-3}(T/K) + 250.068 \cdot 10^3/(T/K)^{-2}$ | 1221 | 17.2 | 110 |
| | | | ($\beta$ phase) 124 | 1114 | 15.8 | |
| $AmCl_3$ | $-977.8 \pm 2.5$ | $146.2 \pm 0.8$ | $81.811 + 41.29 \cdot 10^{-3}(T/K) + 337.81 \cdot 10^3/(T/K)^{-2}$ | 991 | 48.1 | 144 |

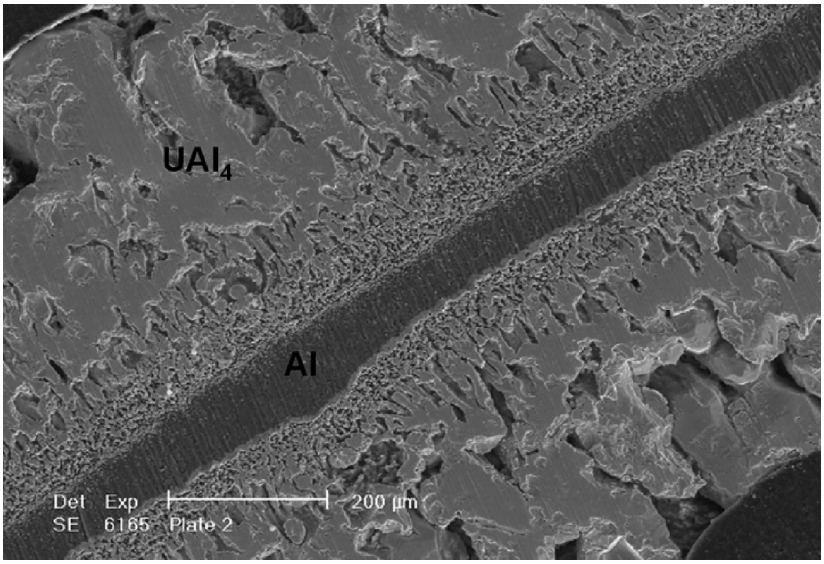

Fig. 1. SEM picture of $UAl_4$ alloy formed on an Al electrode at the interface electrode/molten salt during electrolysis at 450 °C in the LiCl-KCl eutectic.

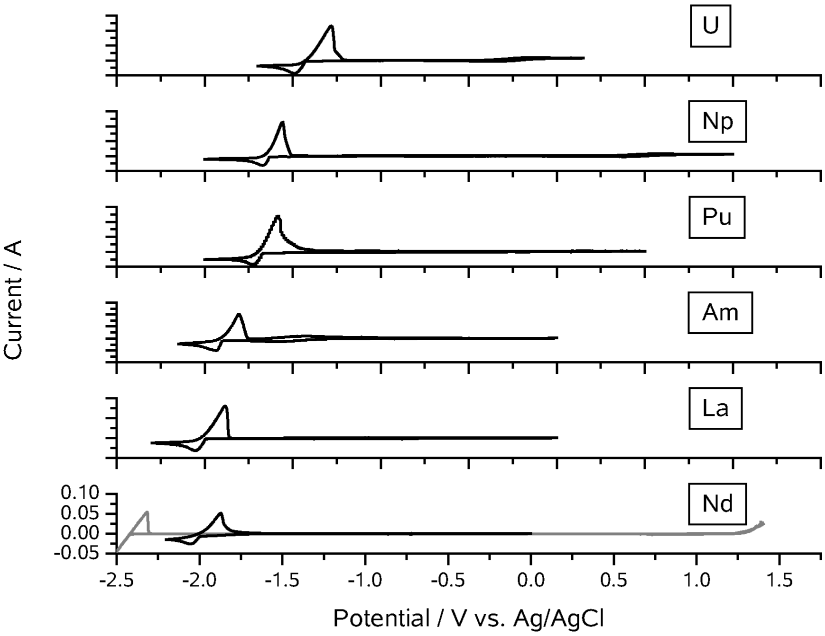

Fig. 2. Comparative cyclic voltammograms obtained on a W electrode for actinides and lanthanides in LiCl-KCl eutectic salt (grey line); T = 733 K; reference electrode Ag/AgCl (1 wt%); [$U^{3+}$] = 9.87 · $10^{-5}$ mol cm$^{-3}$ and $S = 0.34$ cm$^2$; [$Np^{3+}$] = 10.3 · $10^{-5}$ mol cm$^{-3}$ and $S = 0.063$ cm$^2$; [$Pu^{3+}$] = 8.3 · $10^{-5}$ mol cm$^{-3}$ and $S = 0.2$ cm$^2$; [$Am^{3+}$] = 3.65 · $10^{-5}$ mol cm$^{-3}$ and $S = 0.2$ cm$^2$; [$La^{3+}$] = 20 · $10^{-5}$ mol cm$^{-3}$ and $S = 0.19$ cm$^2$; [$Nd^{3+}$] = 70 · $10^{-5}$ mol cm$^{-3}$ and $S = 0.24$ cm$^2$.

### *3.2. Electrochemical Properties on an Al Electrode*

#### $AnAl_4$ Alloy Potential Formation

On an Al electrode the reduction potentials of actinides are more anodic than they are on an inert W electrode. According to the phase diagrams of An-Al systems, e. g. U-Al [27], Pu-Al [27], Np-Al [27], this can be explained by the direct formation of stable $AnAl_x$ alloys at the salt/electrode interface (see Fig. 1: example of a typical $UAl_4$ layer formed on an Al electrode during the electrolysis experiment). Typical cyclic voltammograms are shown in Figure 2. The cathodic branch of the voltammograms corresponds to the formation of the An-Al alloy at the salt/electrode interface whereas the anodic branch is ascribed to the extraction of the actinide from the alloy formed during the cathodic sweep. The potentials of alloy formation between the different actinides and Al

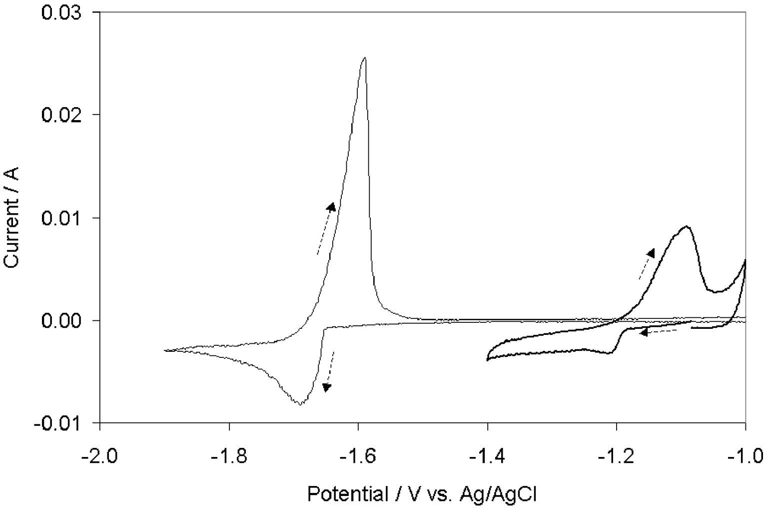

Fig. 3. Comparative cyclic voltammogram of neptunium trichloride in the LiCl-KCl eutectic on a tungsten electrode (simple line) and an aluminium electrode (bold line); counter electrode Mo; reference electrode Ag/AgCl (1 wt%); $T$ = 475 °C (748 K); $S$ = 0.236 cm$^2$; $v = 0.1$ V s$^{-1}$; [Np$^{3+}$] = $2.53 \cdot 10^{-5}$ mol cm$^{-3}$.

Table 5. Derived apparent standard reduction potentials of An on an Al electrode in the LiCl-KCl eutectic at 450 °C.

| Element | $E^{\circ *}_{\mathrm{M(III)/M(Al)}}$ / V vs. Ag/AgCl (1 wt%) | $\Delta G^{\circ}{}_{\mathrm{f}}(\mathrm{AnAl_4})$ / kJ mol$^{-1}$ | Ref. |
|---|---|---|---|
| U | −0.89 | −123.9 | [28] |
| Np | −1.02 | −137.3 | [28] |
| Pu | −1.03 | −164 | [28] |
| Am | −1.08 | −115.7 | [28] |
| Gd | −0.559[a] | −161.81 ($\mathrm{GdAl_3}$) | [29] |
| Er | −0.535[a] | −154.98 ($\mathrm{ErAl_3}$) | [30] |
| Pr | −0.614[a] | −179.92 ($\mathrm{PrAl_3}$) | [31] |

[a] $E$(V) vs. M(III)/M (M = Gd, Er, Pr).

were measured at the crossing of the abscissa and the line formed by the anodic and cathodic branches [25]. On the basis of these voltammograms a graphic determination of the equilibrium potentials $E^{\mathrm{eq}}{}_{\mathrm{M(III)/M(Al)}}$ of each compound is possible, as shown in Fig. 3 for $\mathrm{NpCl_3}$. The values obtained for all actinides are reported in Table 5. They are compared with equilibrium potentials of lanthanides (Ln) taken from the literature. The data clearly confirm that a selective extraction of An is feasible, provided that the reduction potential of the Al electrode is not too negative during the electrolysis process.

### Thermodynamic Properties of $\mathrm{AnAl_4}$ Alloys

To our knowledge the only data available concern $\mathrm{UAl_4}$ and $\mathrm{PuAl_4}$ alloys [27] derived for calorimetric measurements (Fig. 4). The energies of formation of $\mathrm{AnAl_4}$ alloys were calculated at 450 °C from the apparent standard potential according to

$$E^{\circ *}_{\mathrm{M(III)/M(Al)}} = -\frac{\Delta_{\mathrm{r}} G^{\circ}}{3F} - \frac{RT}{F} \ln X_{\mathrm{AgCl}} + \frac{RT}{3F} \ln \gamma_{\mathrm{MCl_3}} . \tag{7}$$

Details of the procedure to determine the thermodynamic data of the $\mathrm{AnAl_4}$ alloys are given in [32].

The thermodynamic properties of $\mathrm{AnAl_4}$ alloys are reported in Table 5 and compared with literature values for $\mathrm{LnAl_4}$ alloys [29–31]. The values obtained range in the same order of magnitude of those of lanthanide-based alloys.

## 4. Conclusions

This work summarizes several experimental investigations of the thermochemical properties of actinides in the LiCl-KCl eutectic. Accurate thermochemical data are reported such as diffusion coefficients, apparent standard potentials and activity coefficients. On the basis of electrochemical measurements, it was shown that the actinide/lanthanide separation can be achieved on an Al electrode whereas the apparent standard potentials of the lower actinides and lanthanides are too close to each other on an inert W electrode. The $\mathrm{AnAl}_x$ alloys formed protect the deposit and prevent the parasit reactions of Am$^{2+}$ with U$^{3+}$, Np$^{3+}$, Pu$^{3+}$ due to the disproportionation reaction of americium metal with Am$^{3+}$ which occurs on a W electrode.

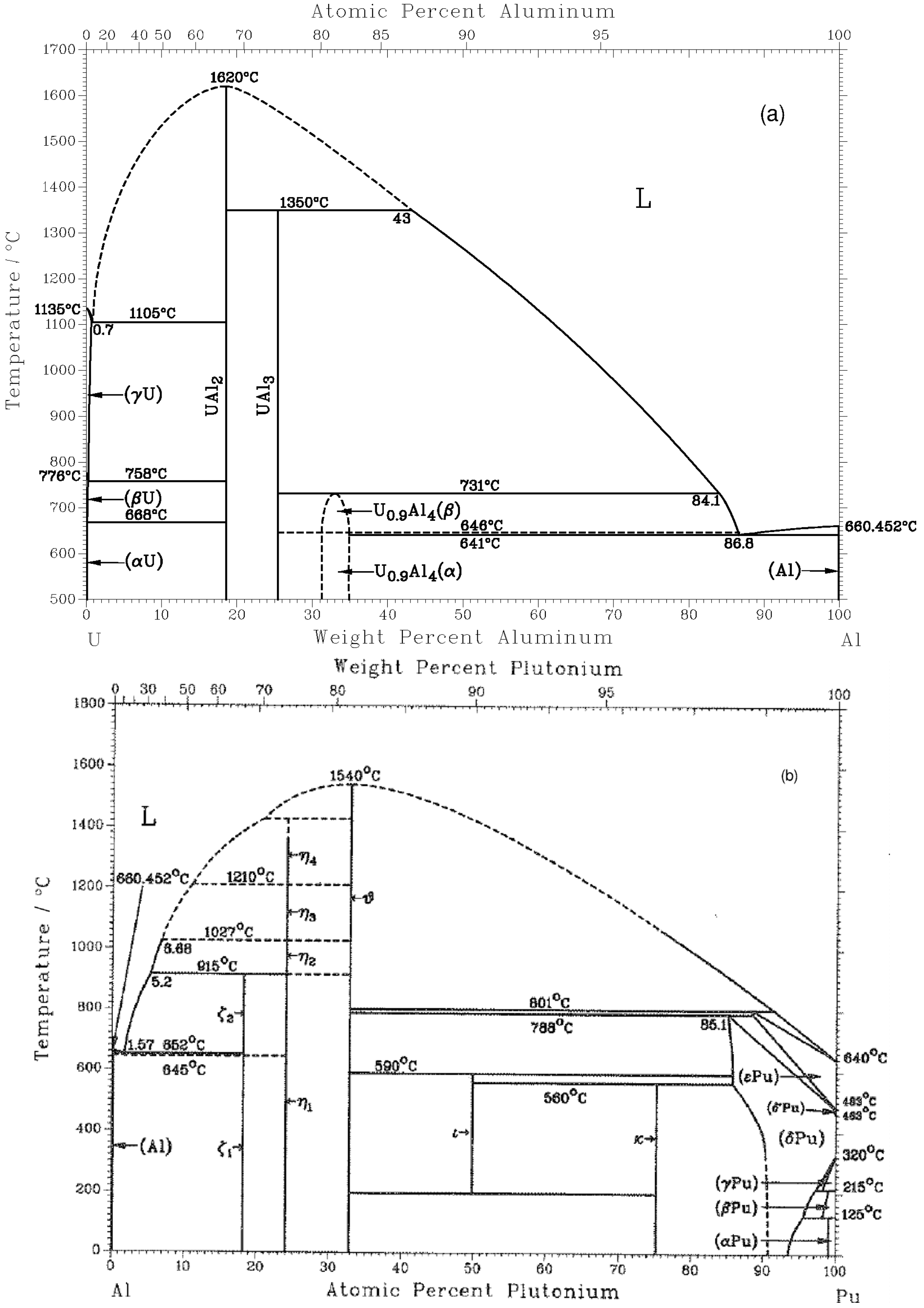

Fig. 4. (a) U-Al and (b) Pu-Al phase diagrams [27].

[1] J. J. Laidler, J. E. Battles, W. E. Miller, J. P. Ackerman, and E. L. Carls, Prog. Nucl. Energy **31**, 131 (1997).

[2] J. Y. Chang, J. Nucl. Mat. **34**, 234 (1997).

[3] Pyrochemical Separations in Nuclear Applications: A Status Report, Report OECD/NEA 5427, Paris, France 2004, p. 175.

[4] P. Masset, P. D. W. Bottomley, R. J. M. Konings, R. Malmbeck, A. Rodrigues, J. Serp, and J.-P. Glatz, J. Electrochem. Soc. **152**, 1109 (2005).

[5] D. A. Nissen, J. Inorg. Nucl. Chem. **28**, 1740 (1966).

[6] D. A. Nissen, Technical Report BNWL-158, Batelle Labs, Richland, WA, USA 1965, p. 8.

[7] L. Martinot, J. Inorg. Nucl. Chem. **37**, 2525 (1975).

[8] K. Serrano and P. Taxil, J. Appl. Electrochem. **29**, 497 (1999).

[9] D. S. Poa, Z. Tomczuk, and R. K. Steunenberg, J. Electrochem. Soc. **135**, 1161 (1988).

[10] J. J. Roy, L. F. Granthman, D. L. Grimett, S. P. Fusselman, C. L. Krueger, T. S. Storvick, T. Inoue, Y. Sakamura, and N. Takahashi, J. Electrochem. Soc. **143**, 2487 (1996).

[11] O. Shirai, J. Alloys. Comp. **271**, 685 (1998).

[12] B. P. Reddy, S. Vandarkuzhali, and P. Venkatesh, Electrochim. Acta **49**, 2471 (2004).

[13] P. Masset, R. J. M. Konings, R. Malmbeck, J. Serp, and J.-P. Glatz, J. Nucl. Mat. **344**, 173 (2005).

[14] J. Serp, R. J. M. Konings, R. Malmbeck, C. Scheppler, and J.-P. Glatz, J. Electroanal. Chem. **561**, 143 (2004).

[15] Y. Sakamura, T. Hijikata, K. Kinoshita, T. Inoue, T. S. Storvick, C. L. Krueger, J. J. Roy, D. L. Grimmett, S. P. Fusselman, and R. L. Gay, J. Alloys Comp. **271 – 273**, 592 (1998).

[16] C. Pernel, Ph.D. thesis, Polytechnic Institute of Grenoble, Grenoble 2002 (in French).

[17] J. Serp, P. Chamelot, S. Fourcaudot, R. J. M. Konings, R. Malmbeck, C. Pernel, J. C. Poignet, J. Rebiznat, and J.-P. Glatz, Electrochim. Acta **51**, 4024 (2006).

[18] D. Lambertin, Ph.D. thesis, University Paris 6, Paris 2002 (in French).

[19] D. Lambertin, S. Sanchez, G. Picard, and J. Lacquement, Radiochim. Acta **91**, 449 (2003).

[20] D. Lambertin, J. Lacquement, S. Sanchez, and G. Picard, Plasmas Ions **3**, 65 (2000).

[21] C. Pernel, J. Serp, M. Ougier, R. Malmbeck, and J.-P. Glatz, Global 2001, Paris, France 2001.

[22] P. Masset, C. Apostolidis, R. Malmbeck, R. J. M. Konings, J. Rebizant, J. Serp, and J.-P. Glatz, J. Electroanal. Chem. **603**, 166 (2007).

[23] O. Shirai, M. Iizuka, T. Iwai, and Y. Arai, J. Appl. Electrochem. **31**, 1055 (2001).

[24] O. Shirai, M. Iizuka, T. Iwai, and Y. Arai, J. Appl. Electrochem. **34**, 323 (2004).

[25] L. Casseyre, R. Malmbeck, P. Masset, J. Serp, P. Soucek, and J.-P. Glatz, J. Nucl. Mat. **360**, 49 (2007).

[26] R. J. M. Konings, The ITU Material Property Data Base for f-Elements and Compounds, f-MPD, 2002. http//www.f-elements.net.

[27] T. B. Massalski, H. Okamoto, P. R. Subramanian, and L. Kacprzak, Binary Alloy Phase Diagrams, 2nd ed., ASM International, Ohio, OH, USA 1990, pp. 156, 178.

[28] P. Masset, M. Malmbeck, J. Serp, and J.-P. Glatz, in preparation.

[29] M. R. Bermejo, J. Gomez, J. Medina, A. M. Martinez, and Y. Castrillejo, J. Electroanal. Chem. **588**, 253 (2006).

[30] Y. Castrillejo, M. R. Bermejo, E. Barrado, and A. M. Martinez, Electrochim. Acta **51**, 1941 (2006).

[31] Y. Castrillejo, M. R. Bermejo, P. Diaz Arocas, A. M. Martinez, and E. Barrado, J. Electroanal. Chem. **575**, 61 (2005).

[32] P. Chiotti, V. V. Akhachinskij, I. Ansara, and M. H. Rand, The Chemical Thermodynamics of Actinide Elements and Compounds, Part 5, The Actinide Binary Alloys, IAEA Vienna 1981, p. 276.